Supplementary Information for Analyst

Development of a molecularly imprinted electrochemical sensor based on (Cu-BTC)-MOF and graphene composite for highly sensitive and selective chloramphenicol detection

Ni Xiang, Suijian Qi, Jinhua Piao*

School of Food Science and Engineering, South China University of Technology, Guangzhou 510641, China

* Corresponding author. Tel: 86-20-87113849; Fax: 86-20-87113849.
E-mail address: jhpiao@scut.edu.cn (J. Piao)

Table of contents

Supplementary information…… ……..……...S3

Scheme S1. Schematic illustration of the synthesis process of (Cu-BTC)-MOF……..….S3

Scheme S2 Schematic illustration of the prepared process of MIP/(Cu-BTC)-MOF/Gr/GCE sensor……. …….……...S3

Fig. S1 SEM images of as-prepared materials: (a) (Cu-BTC)-MOF, (b) (Cu-BTC)-MOF/Gr-1, (c) (Cu-BTC)-MOF/Gr-2, (d) (Cu-BTC)-MOF/Gr-3, (e) (Cu-BTC)-MOF/Gr-4, (f) (Cu-BTC)-MOF/Gr-5..…….…...…S4

Fig. S2 Electrochemical properties of different modified electrodes: (a) CV curves, (b) Nyquist plots……....S5

Fig. S3 (a) CVs of the MIP/(Cu-BTC)-MOF/Gr/GCE sensor measured in the 0.1 M PBS solution (pH 7.0) in a PBS (pH 7.0) buffer solution containing the $[Fe(CN)_6]^{3-/4-}$ redox pair at scan rates range 25-200 mV s^{-1}, (b) Plots of the peak currents *vs*. the square root of scan rates……..……....S5

Fig. S4 Effect of the constructed parameters on the performance of MIP/(Cu-BTC)-MOF/Gr/GCE sensor.……...…S6

Fig. S5 Stability of the MIP/(Cu-BTC)-MOF/Gr/GCE sensor: (a) stability, (b) Long-term stability…….…… …….…… ……...S7

Table S1. The CV peak current for different modified electrodes…… ……. .S7

Table S2 Calculated results of R_{ct} for different modified electrodes…….…...S8

Supplementary information

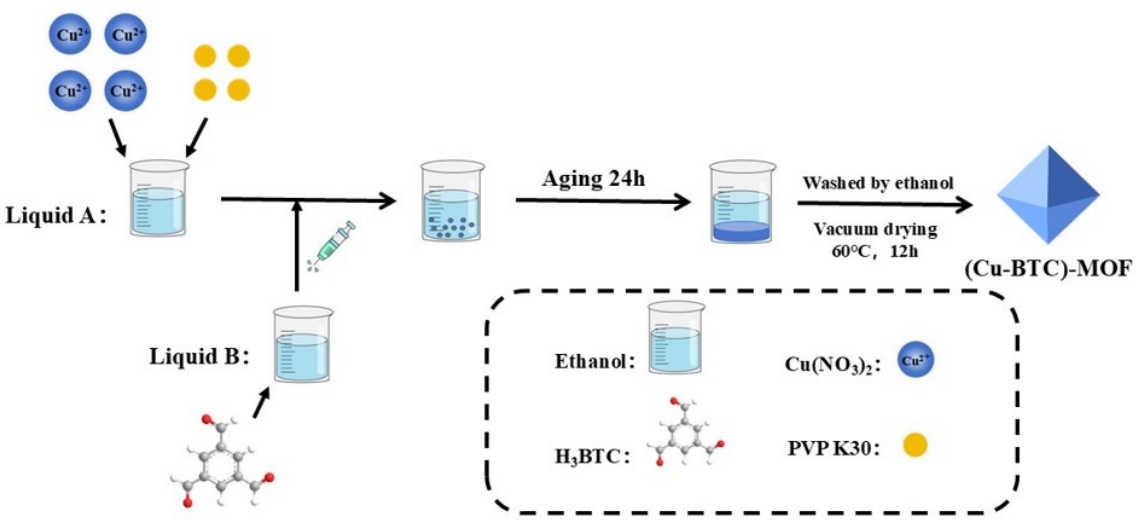

Scheme S1. Schematic illustration of the synthesis process of (Cu-BTC)-MOF.

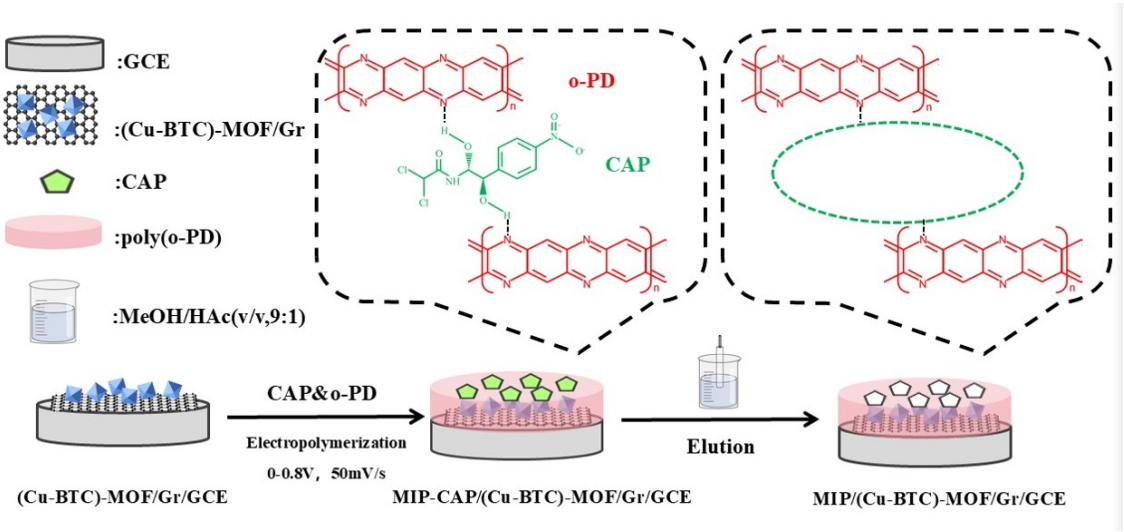

Scheme S2. Schematic illustration of the prepared process of MIP/(Cu-BTC)-MOF/Gr/GCE sensor.

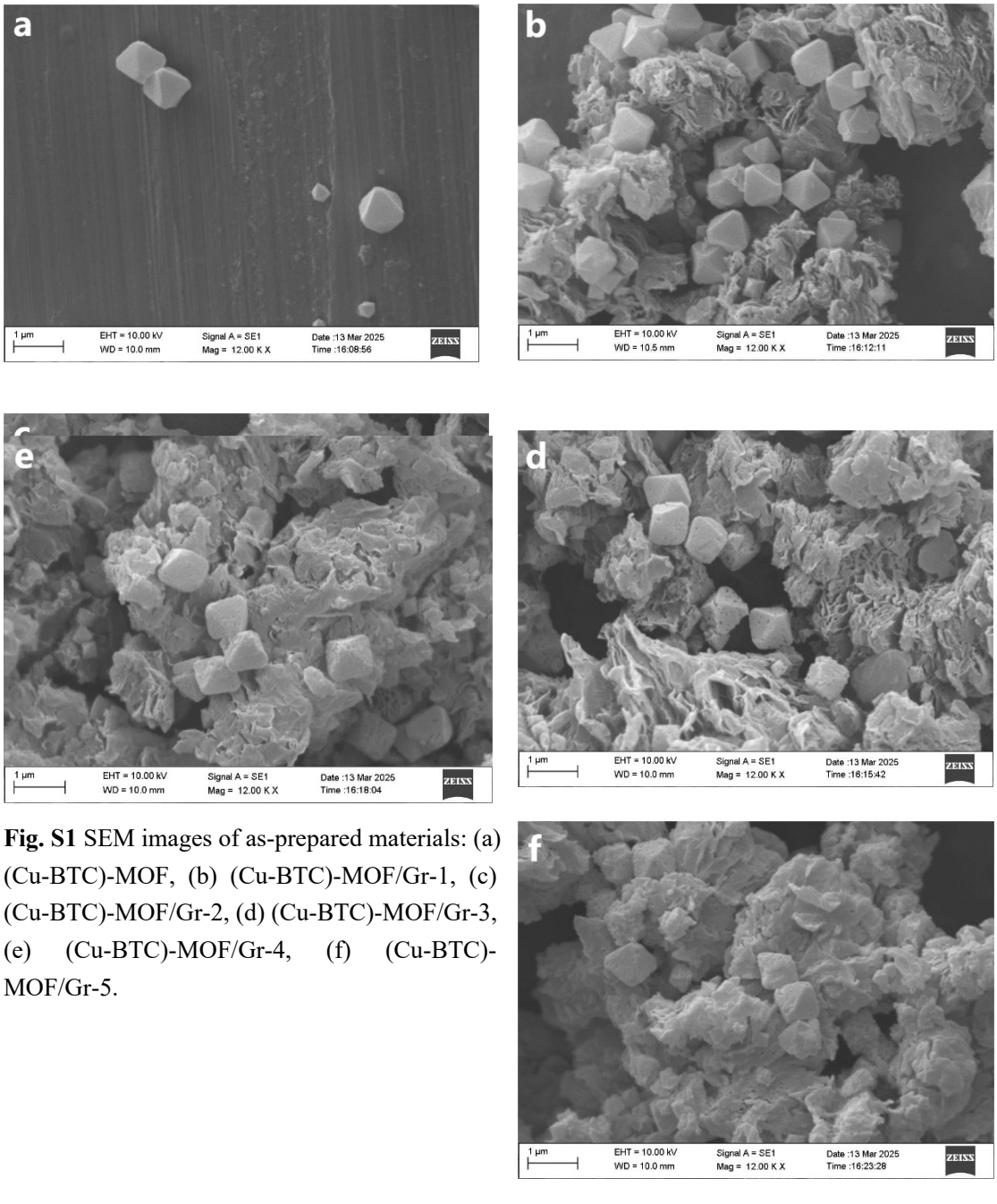

Fig. S1 SEM images of as-prepared materials: (a) (Cu-BTC)-MOF, (b) (Cu-BTC)-MOF/Gr-1, (c) (Cu-BTC)-MOF/Gr-2, (d) (Cu-BTC)-MOF/Gr-3, (e) (Cu-BTC)-MOF/Gr-4, (f) (Cu-BTC)-MOF/Gr-5.

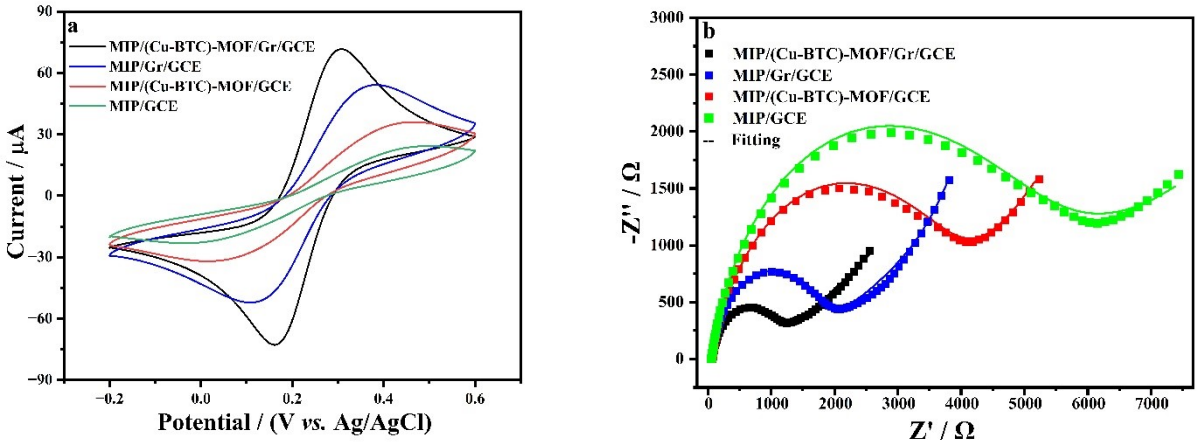

Fig. S2 Electrochemical properties of different modified electrodes: (a) CV curves, (b) Nyquist plots

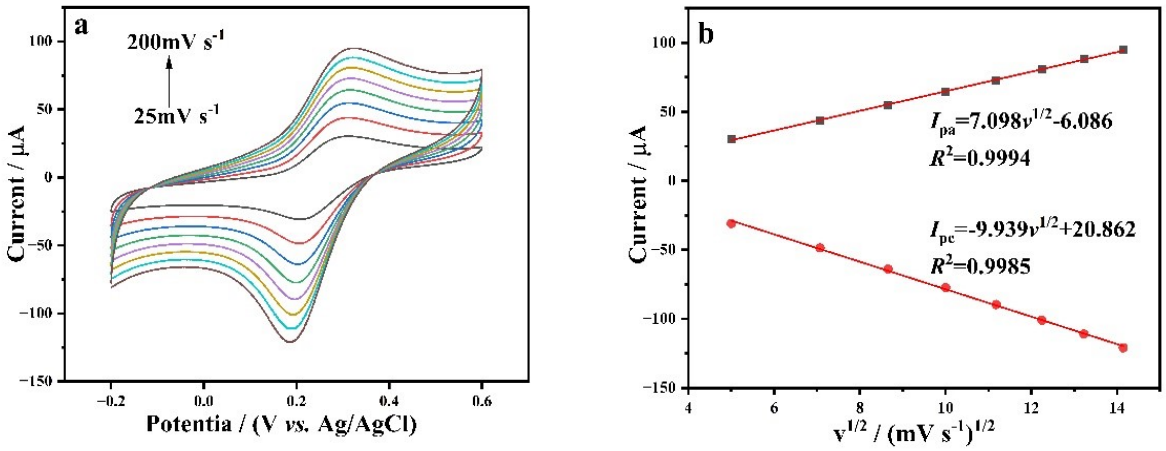

Fig. S3 (a) CVs of the MIP/(Cu-BTC)-MOF/Gr/GCE sensor measured in the 0.1 M PBS solution (pH 7.0) in a PBS (pH 7.0) buffer solution containing the $[Fe(CN)_6]^{3-/4-}$ redox pair at scan rates range 25-200 mV s^{-1}, (b) Plots of the peak currents *vs*. the square root of scan rates.

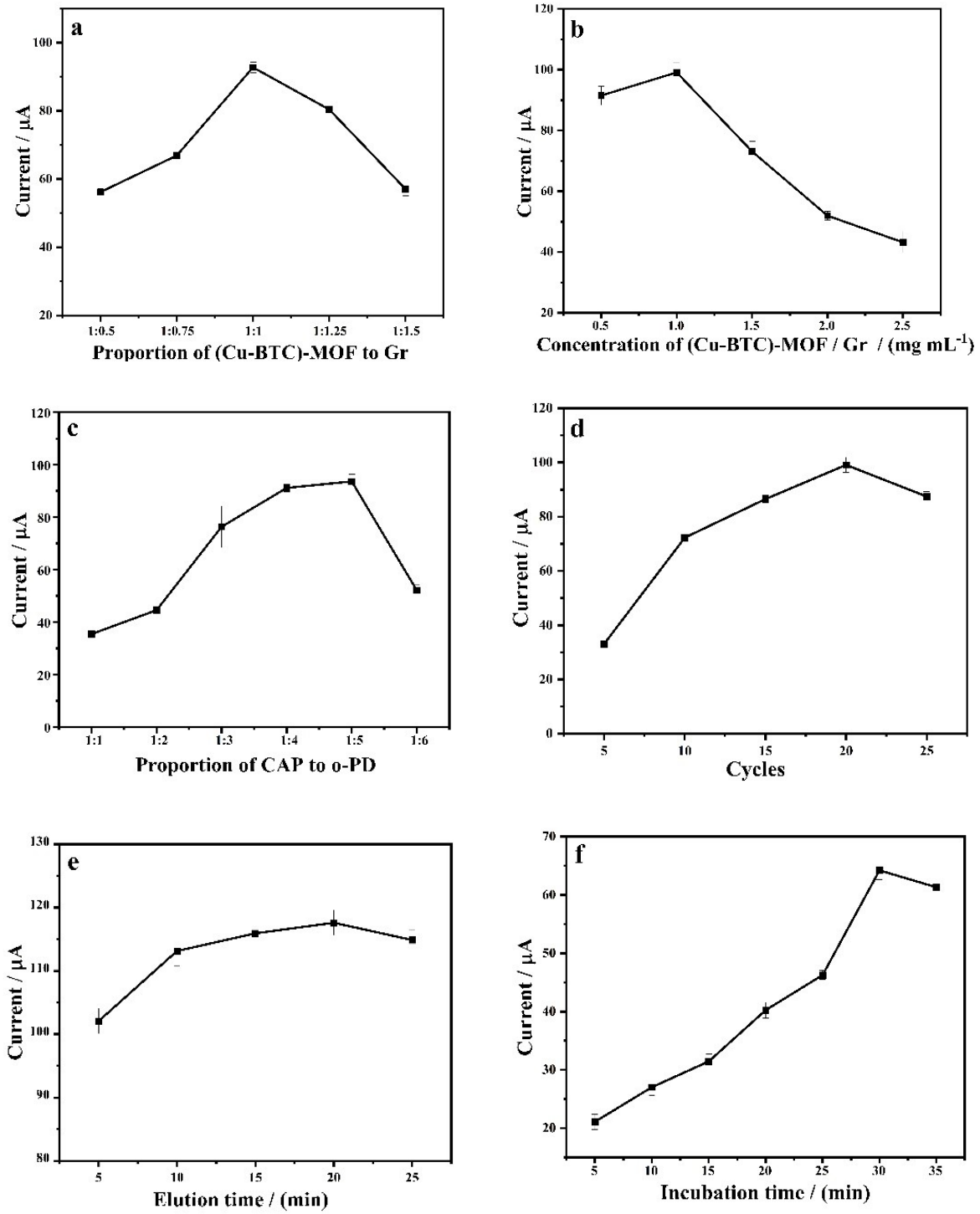

Fig. S4 Effect of the constructed parameters on the performance of MIP/(Cu-BTC)-MOF/Gr/GCE sensor.

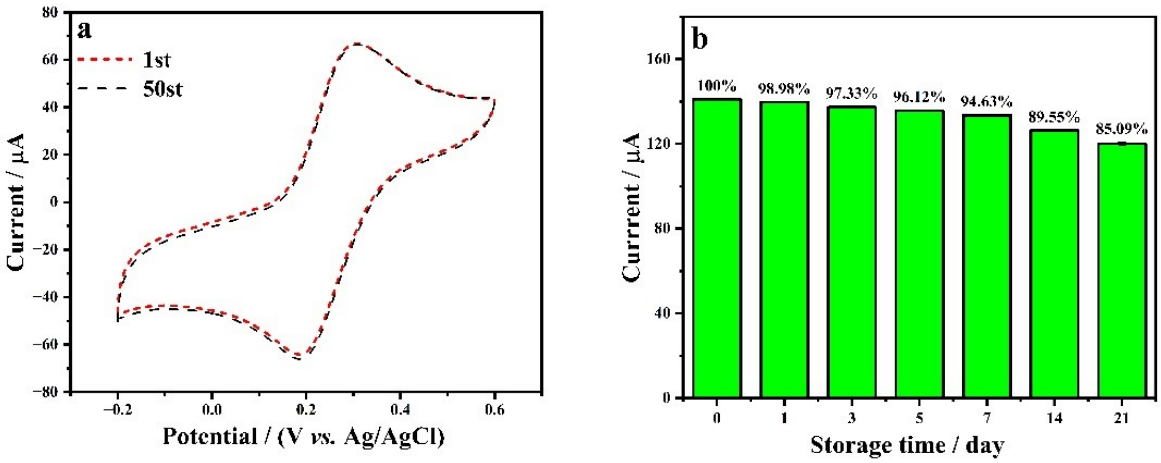

Fig. S5 Stability of the MIP/(Cu-BTC)-MOF/Gr/GCE sensor: (a) stability, (b) Long-term stability.

Table S1 The CV peak current for different modified electrodes

Electrode	*I*/μA
GCE	85.3
(Cu-BTC)-MOF/GCE	42.4
Gr/GCE	216.0
(Cu-BTC)-MOF/Gr/GCE	117.0
MIP/Gr/GCE	54.1
MIP/(Cu-BTC)-MOF/GCE	36.0
MIP/GCE	23.8
MIP-CAP/(Cu-BTC)-MOF/Gr/GCE	31.6
MIP/(Cu-BTC)-MOF/Gr/GCE	71.6
NIP/(Cu-BTC)-MOF/Gr/GCE	18.2

Table S2 Calculated results of R_{ct} for different modified electrodes

Electrodes	R_{ct}/Ω
GCE	297.6
(Cu-BTC)-MOF/GCE	1897
Gr/GCE	55.92
(Cu-BTC)-MOF/Gr/GCE	274.5
MIP/Gr/GCE	1615
MIP/(Cu-BTC)-MOF/GCE	3108
MIP/GCE	4008
MIP-CAP/(Cu-BTC)-MOF/Gr/GCE	3433
MIP/(Cu-BTC)-MOF/Gr/GCE	908.3
NIP/(Cu-BTC)-MOF/Gr/GCE	4552